STEM CELLS TRANSLATIONAL MEDICINE®

TISSUE-SPECIFIC PROGENITOR AND STEM CELLS

Neural Precursor Cell Transplantation Enhances Functional Recovery and Reduces Astrogliosis in Bilateral Compressive/Contusive Cervical Spinal Cord Injury

JARED T. WILCOX,[a,b,*] KAJANA SATKUNENDRARAJAH,[b,*] JEFFREY A. ZUCCATO,[a] FARSHAD NASSIRI,[a] MICHAEL G. FEHLINGS[a,b]

Key Words. Cervical spinal cord injuries • Neural stem cells • Cell transplantation • Forelimb • Tissue preservation • Electrophysiology

[a]Institute of Medical Science, University of Toronto, Toronto, Ontario, Canada; [b]Division of Genetics and Development, Toronto Western Research Institute, University Health Network, Toronto, Ontario, Canada

[*]Contributed equally.

Correspondence: Michael G. Fehlings, M.D., Ph.D., Toronto Western Hospital, 399 Bathurst Street, Toronto, Ontario, M5T 2S8, Canada. Telephone: 416-603-5800, ext. 2182; E-Mail: Michael.Fehlings@uhn.ca

Received February 14, 2014; accepted for publication June 26, 2014; first published online in SCTM *Express* August 8, 2014.

1066-5099/2014/$20.00/0

http://dx.doi.org/10.5966/sctm.2014-0029

ABSTRACT

Spinal cord injury has a significant societal and personal impact. Although the majority of injuries involve the cervical spinal cord, few studies of cell transplantation have used clinically relevant models of cervical spinal cord injury, limiting translation into clinical trials. Given this knowledge gap, we sought to examine the effects of neural stem/precursor cell (NPC) transplants in a rodent model of bilateral cervical contusion-compression spinal cord injury. Bilateral C6-level clip contusion-compression injuries were performed in rats, which were then blindly randomized at 2 weeks after injury into groups receiving adult brain-derived NPCs, vehicle, or sham operation. Long-term survival of NPCs was evident at 10 weeks after transplant. Cell grafts were localized rostrocaudally surrounding the lesion, throughout white and gray matter. Graft-derived cells were found within regions of gliotic scar and motor tracts and deposited myelin around endogenous axons. The majority of NPCs developed an oligodendroglial phenotype with greater neuronal profiles in rostral grafts. Following NPC transplantation, white matter was significantly increased compared with control. Astrogliosis and glial scar deposition, measured by GFAP-positive and chondroitin sulfate proteoglycan-positive volume, was significantly reduced. Forelimb grip strength, fine motor control during locomotion, and axonal conduction (by in vivo electrophysiology) was greater in cell-treated animals compared with vehicle controls. Transplantation of NPCs in the bilaterally injured cervical spinal cord results in significantly improved spinal cord tissue and forelimb function, warranting further study in preclinical cervical models to improve this treatment paradigm for clinical translation. STEM CELLS TRANSLATIONAL MEDICINE *2014;3:1148–1159*

INTRODUCTION

Spinal cord injury (SCI) has significant societal impact, with annual incidence of 30–70 cases per million and 1.3 million persons currently affected in North America [1, 2]. Cervical SCI represents more than 60% of injuries and can incur considerable lifetime socioeconomic costs [3, 4]. Returning function to the hand and upper limb is the primary concern of patients and the primary goal for medical therapies; however, there is a critical lack of studies using clinically relevant models of cervical SCI in preclinical and translational research [5]. Preclinical models of contusion-compression SCI are needed for translating therapies to the clinic [6, 7]. Furthermore, clinical trials using stem cell transplantation for SCI have experienced considerable difficulties [8–10], indicating that preclinical data on recovery of the forelimb in cervical SCI may be critical for successful translation of stem cell therapy.

Traumatic SCI typically consists of bilateral contusion and compression with subsequent secondary injury cascades that exacerbate the injury. Sharp and unilateral injury models (i.e., hemisection and hemicontusion) have limited neuron loss, immune response, and gliotic scarring and exhibit functional deficits regardless of injury level [11–14]. Consequently, preclinical efficacy should be conducted using cervical contusion-compression models demonstrating a dose response toward tissue and neurobehavioral outcomes prior to clinical application of cell therapy [6, 14, 15]. Primary outcomes of therapeutics for SCI include tissue preservation, reduced inflammation and gliotic scarring, increasing neuroplasticity, and some resulting neurobehavioral recovery. The connection between functional recovery and tissue-specific primary outcomes is not well known.

Several endogenous progenitor populations are capable of proliferating and activating

following injury to replace lost tissue and to limit secondary damage [16, 17]. The application of exogenous stem cell transplantation into the injured spinal cord to mimic these repair processes has been thoroughly studied in thoracic SCI [18, 19]. Of the various cell types used for repair of the injured central nervous system, neural stem/precursor cells (NPCs) have demonstrated great promise and repeated efficacy in thoracic SCI models [18]. Transplantation of NPCs has demonstrated advantages for graft-mediated repair, with NPC-derived neuronal or oligodendroglial lineages conferring neuroplasticity or remyelination in some studies of thoracic SCI [20–22]. The efficacy of stem cell transplantation with respect to tissue preservation and lesion reduction in cervical SCI is poorly understood.

Axonal regeneration and neuroplasticity is restricted by oligodendroglial death and dysmyelination as well as by classical physical barriers such as astrogliosis and cavitation [23, 24]. Modest axonal sparing can substantially enhance conduction and limb function because preserving roughly 10% of initial axon number can maintain function [25]. Remyelination of host axons by NPC transplants has been proposed as a critical mechanism of NPC-mediated recovery in thoracic SCI [26–29]. White matter preservation has been reported previously in some thoracic SCI models following transplantation of NPCs and glial-restricted progenitors [26, 30, 31] but not in others [20, 32, 33]. Similarly, astrocyte reactivity and glial scar formation during the secondary injury cascade inhibit regeneration and conduction, precluding functional recovery following SCI [34, 35]. Enzymatic degradation of GFAP and chondroitin sulfate proteoglycan (CSPG) coincides with improved motor function in thoracic SCI [36, 37]; however, cell transplantation has been shown to reduce astrogliosis and scarring [26, 38–40] or upregulate astrogliotic scarring [41, 42], regardless of hind-limb motor improvement. Cell transplantation has been studied previously in bilateral and midline cervical SCI [31, 43, 44]; however, increased forelimb strength or reduced astrogliosis in subacute cervical SCI has not been demonstrated.

Evaluating the efficacy of NPCs to preserve tissue, increase neuron survival, reduce astrogliosis, and improve forelimb function in cervical SCI models could advance cell transplantation therapy for spinal injury. To address these issues, we delivered NPCs into a novel model of cervical SCI in the rat followed by extensive evaluation of neurobehavioral recovery. Long-term survival and engraftment of NPCs in the cervical enlargement were observed, with resulting increased tissue preservation and reduction of astrogliosis. Recovering hand function is the primary concern of persons living with spinal injuries [5]. Understanding of whether cell transplantation ameliorates physiology and function of the upper limb is limited, slowing translation toward human trials [6]. Insight into NPC-mediated recovery in translatable cervical models could address this gap in clinical translation.

Materials and Methods

Animals and Cervical Spinal Cord Injury

Adult Wistar rats of 270–310 g ($n = 60$, Charles River Laboratories, Wilmington, MA, http://www.criver.com) and adult YFP mice ($n = 12$; 129-Tg[ACTB-EYFP]2Nagy/J; Jackson Laboratory, Bar Harbor, ME, http://www.jax.org) were used in all experiments. Experimental protocols were approved by the animal care committee of the University Health Network (Toronto, Ontario, Canada) in accordance with the policies of the Canadian Council of Animal Care for use of experimental animals and under the supervision of clinical veterinarians.

Cervical spinal cord injuries were realized with the extensively validated modified aneurysm clip contusion-compression model [21, 25, 45–47]. The clip was applied at the C6 vertebral level to cause selective deficits to the wrist and paw (supplemental online data) [48]. Wistar rats of 290 $\pm$ 20 g body weight were anesthetized with isoflurane and administered 0.05 mg/kg buprenorphine and 5 ml saline, and a C6 and C7 laminectomy was performed. A modified aneurysm clip calibrated at a 28.1 g (27.6 kdyne) was applied around the cord, allowed to snap shut, and sustained for 60 seconds.

Animals received extensive postoperative care including Clavamox in drinking water 3 days before injury until endpoint and were housed in a 12-hour light-dark cycle at 26°C with ad libitum food and water. Animals were administered buprenorphine (0.1 mg/kg) for 3 days and meloxicam (1.0 mg/kg) for 5 days. Injured rats were administered fluids and nutritional support, and bladders were manually expressed t.i.d. for 14 days and as needed. Exclusion criteria were set a priori and assessed blindly (supplemental online data). Exclusion and mortality occurred after injury ($n = 2$ and $n = 4$, respectively) and after randomization ($n = 1$ and $n = 8$, respectively).

Neural Precursor Cell Culture

Adult NPCs were isolated from mice expressing yellow fluorescent protein (YFP), as described previously [21]. The subventricular zone was isolated and dissociated by trypsin and mechanical trituration to single cell suspension and plated on uncoated tissue culture flasks for 7 days in serum-free medium (SFM) with FGF2 and EGF. Primary neurospheres were propagated and passaged weekly with mechanical dissociation in maintenance medium (SFM plus EGF, FGF2, and heparin). NPCs were used for transplantation at passage 4 if $\geq$90% of those viable were cells and were suspended in maintenance medium (vehicle).

Transplantation

Animals were block randomized, and blinded observers performed testing. Blocks were then selected by a second blinded observer to receive NPC transplantation of 4×10^5 cells per animal ($n = 24$), vehicle injection control ($n = 16$), or laminectomy-only sham ($n = 8$) on day 14 after injury (supplemental online Fig. 1). Minocycline (50 mg/kg s.c.) and cyclosporine A (CsA; 10 mg/kg s.c.) adjuvants were given 3 days prior to transplantation and administered for 10 days and until sacrifice, respectively. For neuron survival and ventral horn atrophy, subsequent experimental groups were included, as described, and received NPC transplantation of 4×10^5 cells per animal ($n = 6$) or vehicle injection control ($n = 6$).

Under isoflurane, rats were placed in a stereotactic frame and administered 0.05 mg/kg s.c. buprenorphine and 5 ml s.c. saline, and injuries were carefully re-exposed. Dissociated NPCs suspended at 50,000 cells/μl were injected intraspinally in four sites 0.5–1.0 mm bilateral to the midline and 2–3 mm rostral and caudal, 2.0 μl each, for a total of 4×10^5 cells per animal. Injections were delivered at 0.5 μl/minute, left to dwell for 3 minutes, and retracted over 2 additional minutes. Injected groups received intrathecal infusion of growth factors 30 μg/ml EGF and FGF2 and 10 μg/ml platelet-derived growth factor-AA (PDGF-AA;

Sigma-Aldrich, St. Louis, MO, http://www.sigmaaldrich.com) in artificial cerebrospinal fluid delivered via osmotic minipump for 7 days, as described previously [21].

Tissue Processing and Lesion Morphometry

Animals were deeply anesthetized with euthanyl (80 mg/kg i.p.) or isofluorane and perfused transcardially with 60 ml ice-cold phosphate-buffered saline (PBS) and 180 ml 4% paraformaldehyde in PBS at 12 weeks after injury. Tissues were postfixed for 24 hours and then cryoprotected in 30% sucrose in PBS for at least 48 hours. Spinal cord segments were embedded, frozen, and stored at −80°C. Cryostat sections were made 20 μm thick along 1.5-cm length centered rostrocaudally at the injury site.

Serial sections were stained with the myelin-selective stain luxol fast blue (LFB) and hematoxylin and eosin (H&E), as described previously (n = 4 per group) [49]. Injury epicenter was determined blindly by LFB and H&E analyses from ±2,160 μm to the epicenter, which is the total extent of lesion following this injury. Unbiased measurements were made with a Cavalieri volume probe using Stereo Investigator (MBF Bioscience, Williston, VT, http://www.mbfbioscience.com) for total area, gray matter, white matter, cavitation, and total lesion reported as percent area and volumes.

Immunohistochemistry and Quantification

Graft length, NPC cell survival, migration, differentiation, and gliotic scar and astrogliosis volumes were performed blindly, as described previously [21, 50]. Slides were air dried, rinsed with PBS for 3 × 5 min, then blocked and permeabilized for 45 minutes at room temperature. Slides were incubated at 4°C overnight with primary antibodies (supplemental online data) recognizing Olig2, PDGFRA, APC, GFAP, βIII-tubulin, ChAT, neuronal nuclei (NeuN), nestin, Ki67, protein kinase C-γ (PKCγ), contactin-associated protein (CASPR), neurofilament 200 (NF200), MBP, and CSPG overnight at 4°C. Slides were rinsed and incubated in appropriate fluorescent secondary antibodies overnight at 4°C with nuclear counterstain.

Cords were rerandomized, and an observer blinded to treatment and behavioral outcomes performed quantitative stereology. Rostrocaudal graft length and differentiation profiles (n = 7) were determined with a 20-μm interval, and sections were imaged at 80- to 240-μm intervals for differentiation using unbiased stereology (MBF Bioscience) with 5–20 guarded counting grids per section with 8–20 sections per cord (n = 7, ≥100 grids per cord). Quantification of MBP, Ki67, and nestin expression in NPCs was determined with 6 animals per group, with >400 cells recorded for each marker. Representative images were taken with a Zeiss LSM 510 confocal laser microscope (Carl Zeiss, Jena, Germany, http://www.zeiss.com) and represent median signal intensity and cell density.

Ventral horn volumes were quantified by a blinded observer via tracing Laminae 7-9 in cross-sectional tissue samples from a second set of experimental animals (NPC transplantation of 4 × 105 cells per animal [n = 6] or vehicle injection control [n = 6]). Areas were measured across five spinal segments, from C6-T2 (±4 mm rostrocaudal) and extrapolated to volume using ImageJ (NIH, Bethsda, MD, http://imagej.nih.gov/ij/). Total neuron and α-motor neuron numbers were generated through analysis of cross-sectional tissue, as described above, across C7-T1 spinal segments (±2 mm rostrocaudal) to correspond to the lesion analysis. Total NeuN-positive ($NeuN^+$) and 4′,6-diamidino-2-phenylindole-positive ($DAPI^+$) neurons in laminae 7–9 and $NeuN^+ChAT^+DAPI^+$ motor neurons in laminae 9 were assessed by a blinded observer and reported as estimated cell number.

Astrocyte reactivity (astrogliosis) and extracellular matrix (ECM) deposition (gliotic scar formation) were determined with GFAP and CSPG reactivity, respectively. Images of whole cross-sections at ≤240-μm intervals were taken with a Leica fluorescence microscope and quantitatively analyzed using Cavalieri-based stereology (Stereo Investigator; MBF Bioscience) for marker-positive area, total tissue, and cavitation. Uninjured control tissue was used for threshold minimum and normalization in the linear histogramatic range.

Behavioral Assessment

All neurobehavioral assessments were performed and analyzed by examiners blinded to treatment groups. Tests were performed once per week for 10 weeks after injury (vehicle, n = 8; NPC, n = 16; sham, n = 3). Animals were block randomized into groups based on grip strength and Basso, Beattie and Bresnahan (BBB) scores 1 day prior to transplantation to eliminate group variation bias and were transplanted and rerandomized. Correlational analysis was performed on animals clustered around the mean of the respective group (n = 4 per group).

Hind-limb function was tested using the 21-point open-field BBB locomotor scale and 13-point modified BBB subscore, as described previously [51]. To assess whole-body limb and trunk motor function, the inclined plane test was performed, as described previously [45]. Rats were placed on a horizontal plane that was pivoted to increase the level of incline from 15° to 90° at increments of 2.5°. The rats were placed with their body axis parallel to the axis of incline and were required to maintain their body position on the raised plane for 5 seconds for ≥3 of 5 attempts.

Forelimbs were specifically tested with a grip strength meter (GSM) for composite paw strength. For grip strength, animals were held by the hind limbs and lower abdomen and drawn backward at a consistent speed within reach of a metal rung connected to a GSM apparatus. Animals grasp the rung reflexively, and a force gauge measures the maximal force achieved when grip is broken; scores were averaged over five successful grasps.

Electrophysiology

Sensory-evoked potentials (SEPs) were recorded from another set of animals that had received NPC or vehicle or from uninjured controls (n = 6 per group) under isoflurane anesthesia immediately prior to humane sacrifice. Rats were placed in a stereotaxic frame prone, and electrodes were placed at C2 extradurally and in the median nerve at the manus. A constant current stimulus of 0.1 millisecond in duration and 2.0 mA in intensity was applied at a rate of 5.7 Hz to the median nerve. At a bandwidth of 10–3,000 Hz, a total of 500 SEPs were averaged and replicated to obtain peak latency and peak amplitudes.

Statistical Analyses

Data were analyzed with SigmaStat and StatPlus using a two-tailed comparison (α = 0.05). Analyses included two-way repeated-measures analysis of variance (ANOVA) with Bonferroni post hoc test (behavioral), Student's t test (lesion and tissue), or one-way ANOVA with Kruskal-Wallis post hoc test (electrophysiology). Pearson's correlation coefficient and Spearman's ρ were

used to determine behavior-to-tissue and behavior-to-graft relation (df = 6). Results are stated in mean ± SEM.

RESULTS

Cervical Contusion-Compression Spinal Cord Injury Model

Based on previous studies in our laboratory, we sought to generate a cervical model that allowed for forelimb-specific deficits within a therapeutic window. The clip contusion-compression applied at the C6 vertebral level calibrated to 28 g of closing force satisfied these parameters (Fig. 1A; supplemental online Fig. 1). The C6 model delivered a reliable lesion with hallmark lesional tissue and cavitation, appearing as fluid-filled syrinx, in the central spinal tissue. Vehicle-treated animals had no surviving gray matter at the lesion epicenter, whereas NPC-administered animals retained negligible (<5%) viable gray matter. Preserved white matter was evident at the lesion epicenter in the subpial periphery but was markedly decreased compared with uninjured controls. This pattern of central spinal cord tissue loss results in distinct sensorimotor deficits in at-level forelimb and forepaw functions versus below-level hind-limb functions.

No pial rupture or spinal root distraction was observed following initial surgery (n = 48). At 2 weeks after injury, during the subacute phase of secondary injury, cells or vehicle were injected into four sites intraspinally (Fig. 1A). With a strict intraspinal injection procedure consisting of long dwell time and staged needle withdrawal, neither backflow nor bruising was observed. Mortality within this study was 10% (n = 4) prior to randomization at 2 weeks and 20% (n = 8) following randomization up to 12 weeks after injury. The total exclusion rate was not different between vehicle- and adult NPC-treated groups, and fastidious postoperative care greatly reduced occurrence of morbidity such as digit autotomy, spasticity, respiratory distress, and cachexia.

Neural Precursor Cell Engraftment and Differentiation

We then used the C6 contusion-compression model to determine the efficacy of cell transplantation therapy following cervical SCI. Adult NPCs readily engrafted when delivered into the subacutely injured cervical spinal cord via intraspinal injection, surviving to the long-term endpoint at 10 weeks (Fig. 1B). Cells engrafted at 2 weeks after injury localized to the perilesional rostrocaudal tissue and exhibited typical cell morphology. Cells were found in gray and white matter along the dorsoventral axis but were uncommon within the lesion epicenter. Adult NPCs survived to 10 weeks after transplantation (week 12) with low-dose CsA immunosuppression, exhibiting a mixed differentiation profile (Fig. 1C).

Next, we determined the differentiation profiles of surviving grafted cells. The majority of NPC-derived cells were of oligodendroglial lineage, with 49.0 ± 2.3% exhibiting Olig2$^+$ pan-oligodendroglial immunophenotypes and 34.6 ± 2.1% showing an APC$^+$Olig2$^+$ mature oligodendrocyte state. Of the remaining NPCs, 6.2 ± 1.1% were GFAP$^+$ astrocytes, 6.0 ± 1.5% expressing βIII-tubulin were neuronal phenotypes (TUJ1), and 14.2 ± 1.7% expressed YFP alone (Fig. 1D). In the cervical enlargement, YFP$^+$ graft cells and progeny were observed in mixed topographical regions of neurons and glia (Fig. 1C, arrowheads) interspersed with endogenous counterparts (arrows). We then compared the grafts within the cervical enlargement (rostral) with the grafts at the cervicothoracic transition (caudal) to determine regional

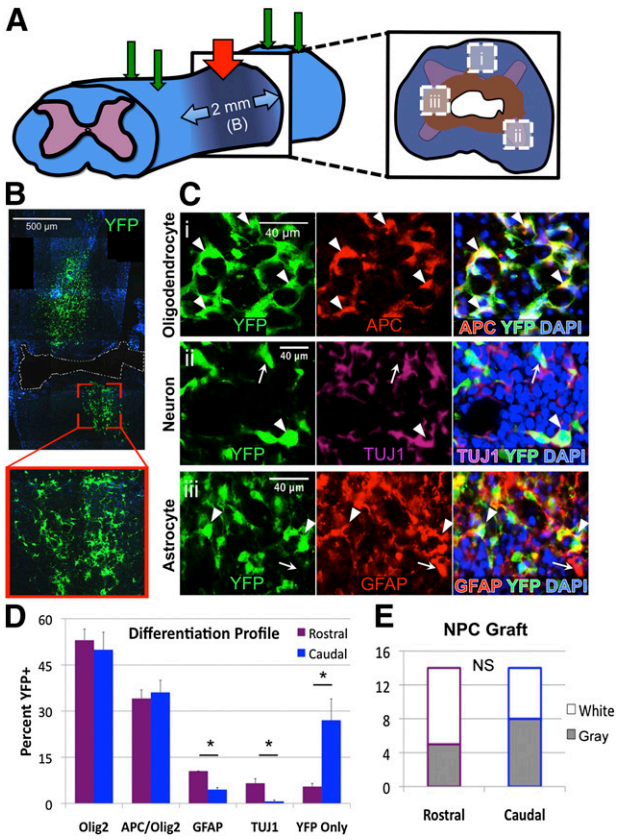

Figure 1. Adult NPCs readily differentiate and engraft in the injured cervical spinal cord. **(A):** Schematic of the experimental design including 28-g cervical spinal cord injury at C6 (red arrow) and four NPC transplantation sites (green arrows). **(B):** Transplanted adult NPCs engraft within the injured cervical cord with long-term survival and cellular processes and morphology typical of NPC-derived progeny. **(C):** Differentiated NPCs and progeny (arrowheads) engraft and intersperse with endogenous cells (arrows) at 10 weeks after transplant. Transplanted cells differentiate to express markers of mature oligodendrocytes **(Ci)**, neurons **(Cii)**, and astrocytes **(Ciii)** (as shown in **[A]**). **(D):** Differentiation profiles of grafted cells at 10 weeks after transplant exhibit a majority of oligodendroglia (49.0%) and mature oligodendrocytes (34.6%), with neurons and astrocytes identified more in the rostral versus caudal region (6.6% vs. 0.7% neurons and 10.5% vs. 4.5% astrocytes). **(E):** The total YFP$^+$ grafts observed on long-term follow-up indicate no difference between rostral and caudal regions within white matter (open) or gray matter (shaded). *, $p < .05$; NS, $p > .05$. Abbreviations: DAPI, 4′,6-diamidino-2-phenylindole; NPC, neural stem/precursor cell; NS, not significant; TUJ1, neuronal βIII-tubulin; YFP, yellow fluorescent protein.

effects on differentiation. The number of cells differentiating into GFAP$^+$ and TUJ1$^+$ cells was significantly higher in the rostral region (10.5% versus 4.5% and 6.6% versus 0.7%, respectively; $p < .05$). Conversely, significantly more unlabeled YFP-only cells were found in the caudal region (27.0% versus 5.5%; $p < .05$), which correlated to the length of NPC grafts in the caudal region (r = .813, p = .026). No difference was observed between the numbers of grafts in regions rostral or caudal to the lesion epicenter (n = 14), and there was not a significant difference in grafts found within white or gray matter in either region (Fig. 1E).

Graft Integration and Tissue Preservation

Following gross localization of the grafts, we examined the microenvironments in which NPCs reside and the resulting effects on

tissue. This further neuroanatomical analysis revealed NPC integration within motor tracts and astrogliotic scarring in the chronically injured cord (Fig. 2). Transplanted YFP$^+$ cells were observed within the dorsal corticospinal tract, with NPCs diffusely integrated with endogenous TUJ1$^+$ neurons within PKCγ^+ regions of dorsal white matter (Fig. 2A). Grafted cells exhibit close localization with apparent cell-cell contact, with enlarged and swollen neuronal processes within these motor tracts. Deposition of myelin is also evident by colocalization of YFP and MBP in close apposition to endogenous NF200$^+$ axons (Fig. 2B) and in proper association and close apposition with CASPR$^+$ nodal myelin structures (Fig. 2C). A high proportion of NPCs expressing Olig2 deposit myelin, with 32.9 $\pm$ 6.4% exhibiting colocalization of MBP$^+$ and YFP$^+$ cells (Fig. 2D). Few YFP-only cells were observed to express nestin (0.5%), as reported previously, and no YFP$^+$ cells were found to express Ki67 (Fig. 2E, 2F). Specific localization patterns to white or gray matter were not evident in the rostral versus caudal regions, although more neuronal differentiation profiles were seen in the rostral cord (Fig. 1D).

Histomorphometric analysis of the total preserved tissue and lesion volumes were performed using LFB- and H&E-stained sections with a rostrocaudal extent of $\pm$2,160 μm from the lesion epicenter (Fig. 3). More white matter was present in NPC-treated animals compared with the vehicle group (62.3 $\pm$ 4.7% versus 50.4 $\pm$ 8.5%, respectively; $p < .05$) (Fig. 3A). Gray matter and cavity volumes were not different between groups ($p = .81$ and $p = .58$, respectively) (Fig. 3B). The difference in lesional tissue between NPC and vehicle groups (3.8 $\pm$ 0.9% versus 12.9 $\pm$ 5.1%) was not statistically significant ($p = .129$); however, the effect size and potential biological significance observed (Fig. 3C, 3D) led to closer analysis of the change in lesional tissue following NPC transplantation.

Quantification of preserved ventral horn volumes (laminae 7–9) was then performed spanning C6–T2 spinal segments, representing the total forelimb motor pool. This analysis revealed larger volumes in NPC-transplanted animals (12.4 $\pm$ 0.8 mm versus 10.8 $\pm$ 0.3 mm); however, this did not reach significance ($p = .10$). Ventral horn volumes across spinal segments demonstrating lesional tissue (segments C7–T1, $\pm$2,160 μm rostrocaudal) showed similar results (6.2 $\pm$ 0.6 mm versus 5.2 $\pm$ 0.3, NPC versus vehicle; $p = .14$). We next quantified total neuron and α-motor neuron preservation across the C7–T1 spinal segment ($\pm$2,160 μm rostrocaudal). Similar to ventral horn atrophy, there was a nonsignificant trend toward greater total NeuN$^+$ neurons and ChAT$^+$ α-motor neurons in NPC-transplanted animals compared with controls (28,480 $\pm$ 3,520 versus 22,464 $\pm$ 2,939 [$p = .22$] and 3,989 $\pm$ 287 versus 2,901 $\pm$ 551 [$p = .11$], respectively). Further analysis was performed to elucidate potential mechanisms beyond tissue preservation.

Astrogliosis Reduction Following NPC Engraftment

Following the reduction in lesional tissue, an analysis of molecular changes in the lesion was performed. Transplanted cells exhibited prevalent engraftment in areas of astrocytosis and gliotic scar at the lesion epicenter and surrounding parenchyma (Fig. 4A). Within sites of high engraftment, endogenous and NPC-derived astrocytes appeared to be less reactive, with smaller somatic bodies and more spindle-like processes. The expression of GFAP and the ECM component CSPG were used to evaluate glia reactivity and ECM deposition, termed "gliotic scarring" (Fig. 4B). The total volume of tissue immunopositive for GFAP across the entire lesion decreased from 9.6 $\pm$ 1.0% to 5.7 $\pm$ 0.7%, or from 2.4 $\pm$ 0.4 mm^3 to 1.4 $\pm$ 0.2 mm^3, in vehicle controls with NPC transplantation ($p < .05$) (Fig. 4C). The total volume of CSPG immunopositive tissue similarly reduced from 7.7 $\pm$ 0.6% to 5.2 $\pm$ 0.5%, or from 1.9 $\pm$ 0.2 mm^3 to 1.3 $\pm$ 0.1 mm^3 ($p < .05$), in vehicle controls compared with NPC-treated animals (Fig. 4E).

A further volumetric analysis was performed to identify the proportion of astrogliosis in the parenchyma that was not contiguous with the lesional cavity. Assessment of parenchymal astrogliosis, the region of transplantation, is less likely to be due to global or nonspecific effects. The tissue expression of GFAP and CSPG in the parenchyma (Fig. 4D) was reduced to less than half that in the NPC-treated group compared with vehicle control, from 3.7 $\pm$ 0.9% to 1.5 $\pm$ 0.2% for GFAP ($p < .05$) and from 2.1 $\pm$ 0.3% to 1.0 $\pm$ 0.1% for CSPG ($p < .01$) (Fig. 4F). Interestingly, parenchymal GFAP and CSPG were not correlated to preserved white matter ($p = .94$ and $p = .49$, respectively), gray matter ($p = .90$ and $p = .89$, respectively), or cavitation ($p = .52$ and $p = .77$, respectively). In fact, total GFAP$^+$ and CSPG$^+$ volumes exhibited no correlation to lesional tissue volumes determined by histopathology ($p = .96$ and $p = .92$, respectively) and were independent of global tissue sparing. Volumetric evaluation of GFAP reactivity and CSPG deposition in the ECM appear to be robust independent measures and are reduced in animals that receive NPC transplantation.

Forelimb Function Was Improved Following NPC Transplantation

Functional sensorimotor improvement was evaluated to determine the efficacy of NPC transplantation in this cervical contusion-compression model. A series of sensorimotor tests specific to forelimb, hind-limb, or global motor performance was performed. Importantly, bilateral C6 contusion-compression caused significant tetraplegia, precluding the use of behavioral tests that require animals to rear or sit and manipulate food. The forelimbs of animals in NPC and control groups exhibited no discernible differences with respect to spasticity and rigidity noted by blinded observers. The forelimb grip strength of NPC and vehicle groups demonstrated consistent improvement, reaching divergent plateaus at approximately 6 and 9 weeks, respectively, after injury but did not reach the strength of sham-operated controls (1073 $\pm$ 43 g; $p < .001$). Significant improvements in the grasp output of NPC-treated animals were observed, reaching strength of 376 $\pm$ 50 g at 10 weeks after injury compared with vehicle-treated peak strength of 203 $\pm$ 48 g ($p < .05$) (Fig. 5A). The inclined plane test, developed to assess the recovery of hind-limb and trunk function in animals without forelimb deficits, did not detect differences in postural stability or global motor function between groups (Fig. 5B). Both NPC and vehicle groups regained the ability to walk with weight-bearing stepping by week 6; however, the BBB scale and subscore did not detect a difference between groups (Fig. 5C, 5D).

Transplantation of NPCs Conferred Improved Cervical Conduction and Physiology

Electrophysiology was performed to substantiate the behavioral findings by determining the integrity and conduction of the spinal cord specific to forelimb innervation. Evaluation of SEP at the

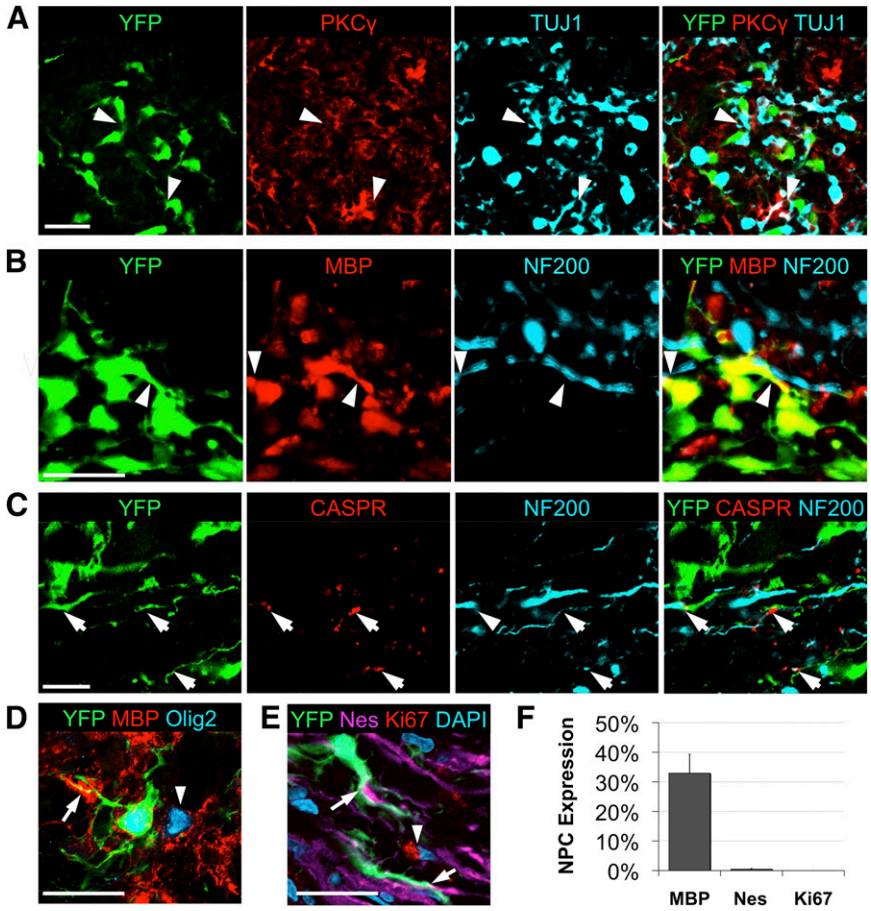

Figure 2. Adult NPCs grafted into cervical spinal cord injury deposit myelin within motor tracts and confer white matter preservation. **(A):** Transplanted YFP$^+$ cells were observed within white matter and motor tracts, with NPCs diffusely integrated with endogenous TUJ1$^+$ neurons (arrowheads) within PKCγ^+ regions of dorsal corticospinal tracts. **(B):** Deposition of myelin is also evident by colocalization of YFP and MBP in close apposition to endogenous NF200$^+$ axons (arrowheads). **(C):** Graft cells were observed at CASPR$^+$ juxtaparanodal regions of compact myelin with normalized spatial molecular channel distribution (arrow). **(D):** Grafted NPCs readily produce MBP (arrow) within areas of endogenous oligodendroglial myelin (arrowhead). **(E, F):** YFP was found to rarely colocalize with the undifferentiated phenotypic marker nestin (arrow), and no Ki67+ proliferative marker expression (arrowhead) was observed in YFP$^+$ NPCs (quantification in **[F]**, $n = 6$). Scale bar = 20 μm. Abbreviations: CASPR, contactin-associated protein; DAPI, 4′,6-diamidino-2-phenylindole; Nes, nestin; NF200, neurofilament 200; NPC, neural stem/precursor cell; PKCγ, protein kinase C-γ; TUJ1, neuronal βIII-tubulin; YFP, yellow fluorescent protein.

forelimb footpad was used to indicate caliber and density of myelinated axons (Fig. 6A, 6B). The SEPs confirmed poor conduction in injured animals compared with sham-operated controls, with latency increasing from 1.25 $\pm$ 0.02 milliseconds to 1.50 $\pm$ 0.05 milliseconds ($p < .01$) and amplitude dampened from 21.55 $\pm$ 1.58 μV to 6.94 $\pm$ 0.98 μV ($p < .001$). These physiological deficits were ameliorated in the NPC-treated animals as latency was returned to values similar to sham animals (1.34 $\pm$ 0.07 milliseconds versus 1.25 $\pm$ 0.02 milliseconds; $p = .29$) (Fig. 6C). Conduction amplitude was significantly increased in the NPC group compared with injured controls (10.39 $\pm$ 2.06 μV vs. 6.94 $\pm$ 0.98 μV; $p < .05$) but remained lower than sham-operated controls ($p < .05$) (Fig. 6D). Similar to grip-strength performance, the sensory physiology of the forelimb-related cervical cord was partially ameliorated following NPC transplantation.

Considering these results, further effort was made to elucidate the relationship among cell engraftment, tissue status, and behavioral performance (supplemental online Table 1). The total length of NPC graft was directly proportional to increased grip strength ($r = .83$, $p = .02$) at 10 weeks after injury (Fig. 7A). A strong positive correlation was also observed between grip strength and white matter preserved ($r = .81$, $p = .02$) (Fig. 7B), with a concomitant negative relationship to total lesion ($r = -.89$, $p < .01$) and weak negative correlation to total CSPG$^+$ tissue volume ($r = -.65$, $p = .08$) (Fig. 7C, 7D). Of note, grip strength was not correlated with preserved gray matter, total cord volume, or cavitation ($p = .76$, $p = .72$, and $p = .10$, respectively), which were not significantly improved following NPC transplantation. BBB scores were proportional to preserved white matter ($r = .76$, $p = .03$) (Fig. 7C) but not to lesion volume, NPC graft length and location, or astrogliosis ($p = .23$, $p = .29$, and $p = .18$). It is important to note that most animals had reached the ceiling effect with BBB scores of 11 (77% NPC, 60% vehicle; $p = .47$), which limits the value of correlational analyses with discrete BBB scores. Interestingly, BBB subscores did not show any relation to white matter sparing ($p = .86$) but exhibited a strong correlation to NPC graft length and number of grafts localized to the lateral white matter ($r = .92$, $p < .01$; $r = .81$, $p = .03$, respectively). Lastly, inclined plane measures were not significantly correlated to tissue preservation or NPC engraftment.

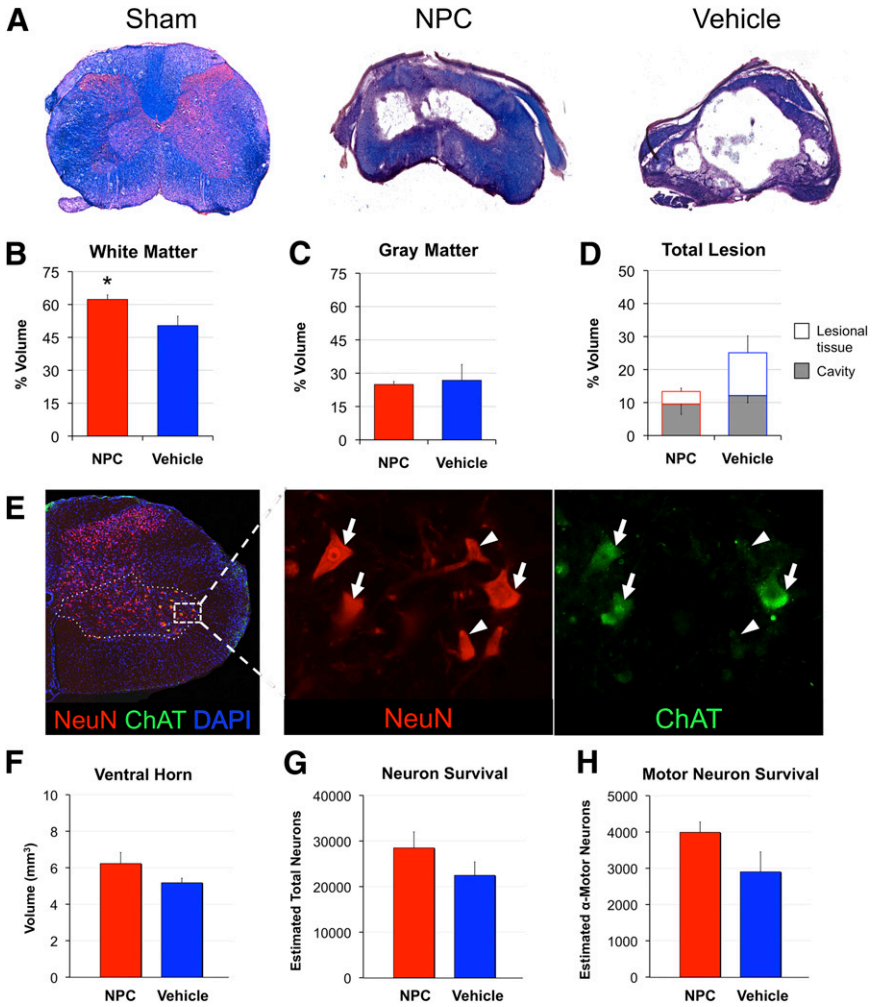

Figure 3. Neural precursor cell transplantation in subacute cervical spinal cord injury confers white matter preservation. **(A):** Cross-sectional tissue stained with luxol fast blue and hematoxylin and eosin reveals a severe, bilateral lesion epicenter at C6 with spared circumferential tissue in NPC- and vehicle-treated groups. **(B, C):** More white matter was present in NPC-treated animals compared with the vehicle group (62.3% vs. 50.4%) **(B)**, whereas gray matter was not different **(C)**. **(D):** Lesion morphometry of NPC versus vehicle groups demonstrates no difference in cavitation (open) and nonsignificant decrease in lesional tissue (shaded; 3.8% vs. 12.9%, respectively; $p = .09$). **(E):** Assessment of ventral horn atrophy (dashed line), neuron (arrowhead), and α-motor neuron loss (arrow) was performed to assess specific motor preservation. **(F–H):** There were no statistically significant differences following NPC transplantation despite greater size of ventral horn volume **(F)** and larger number of α-motor neurons **(G)** and total neurons **(H)** remaining. $*$, $p < .05$. Abbreviations: DAPI, 4′,6-diamidino-2-phenylindole; NeuN, neuronal nuclei; NPC, neural stem/precursor cell.

Discussion

Evaluating potential therapeutics in cervical models has been declared as a major translational priority, with a current lack of preclinical studies [6, 18]. In order to address this, we evaluated the effect of NPC-mediated recovery in a novel cervical contusion-compression injury. In this study, we demonstrate that delayed transplantation of NPCs mediates forelimb functional improvements following cervical SCI. Volumetric stereology showed increased white matter preservation and reduction of astrogliosis and ECM scar deposition. Cell transplantation within the complex cervical enlargement also revealed a rostral differentiation gradient and targeted scar reduction in the parenchyma. Functional improvement in grip strength was strongly associated with NPC graft length and tissue preservation and weakly associated with gliotic scar reduction. This study provides novel and robust evidence of forelimb neurobehavioral recovery following contusion-compression injury and the first evidence of NPC-mediated gliotic scar reduction in the injured cervical enlargement. Responding to the stated need for translatable preclinical studies, our data support the timely transition toward cell therapy in cervical contusive-compressive models of SCI.

Modeling Human Spinal Injury

Sharp injury models, such as hemisection/transection and funiculotomy, are highly variable and do not properly model gliotic scarring and cavitation in human injury [11, 14, 52, 53]. Extent of dysmyelination, neuron loss, immune cell infiltration, and necrosis are also greatly attenuated in hemisection injuries compared with contusion models [11]. Forelimb motor function appears to be independent of the level of injury in hemisection models, making translation to human clinical populations problematic [54, 55]. Contusion models of SCI are more indicative of secondary

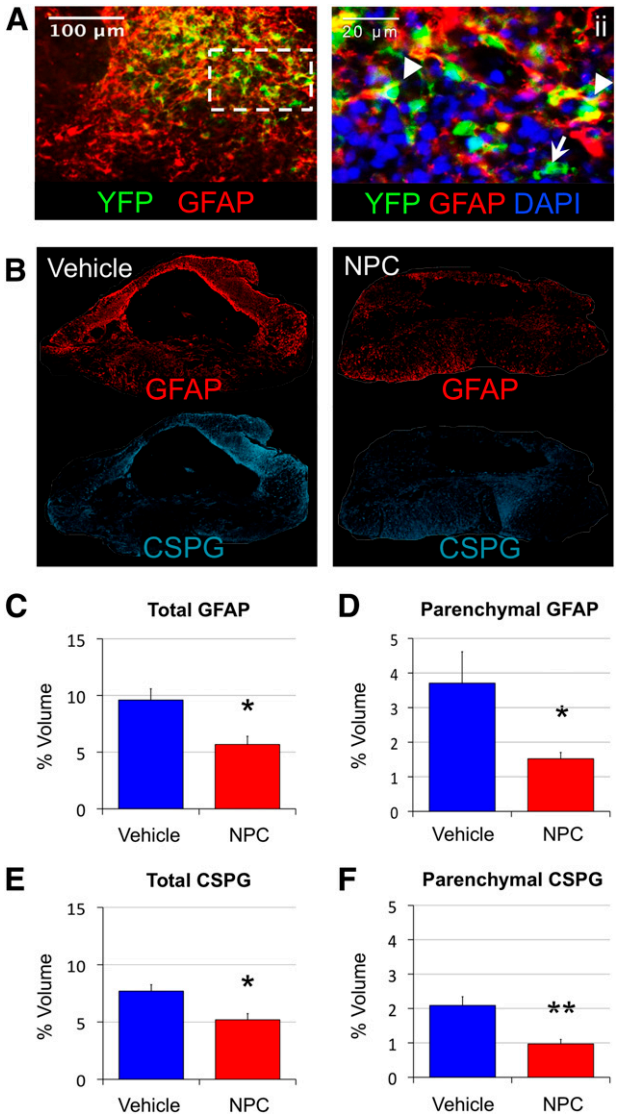

Figure 4. Reactive astrocytosis and glial scar deposition are reduced following NPC transplantation in cervical spinal cord injury. Adult NPCs readily engraft within areas of the gliotic scar **(A, B)** and confer reduced GFAP$^+$ astrogliosis **(C, D)** and CSPG deposition **(E, F)** at 12 weeks after injury. Transplanted cells closely associate with endogenous astrocytes and exhibit astrocyte phenotypes (arrowhead) and nonglial phenotypes (arrow; ii). **(B):** Presence of reactive astrocytes (GFAP) and scar-related CSPG clearly designate gliotic scarring and greater expression in the vehicle group (top) compared with the NPC-treated group (bottom). **(C, E):** Tissue volumes expressing gliotic GFAP and inhibitory CSPG exhibit a statistically significant decrease in NPC animals compared with vehicle controls. **(D, F):** Further volumetric analysis demonstrates that the significant decreases of total GFAP$^+$ and CSPG$^+$ tissue are largely due to reduction of the parenchymal proportion of astrogliotic scarring. $*$, $p < .05$; $**$, $p < .01$. Abbreviations: CSPG, chondroitin sulfate proteoglycan; DAPI, 4′,6-diamidino-2-phenylindole; NPC, neural stem/precursor cell; YFP, yellow fluorescent protein.

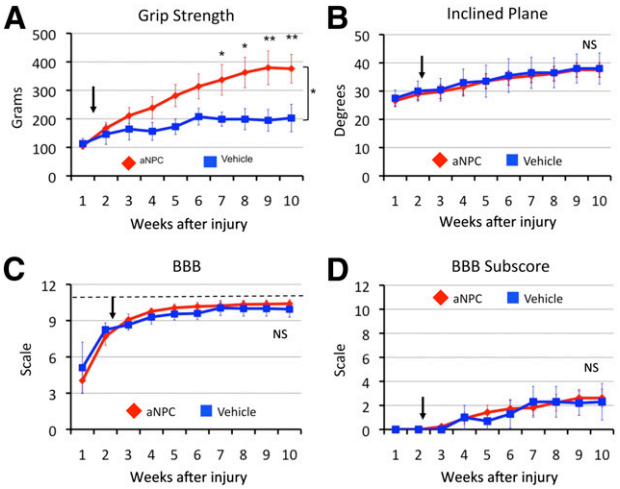

Figure 5. Behavioral improvement was observed in forelimbs following transplantation of neural precursor cells. **(A):** Cervical spinal cord injury caused severe deficit in forelimb grip strength that improved progressively across 10 weeks after injury. Grip strength following NPC transplantation (arrow) was markedly improved compared with and reached plateau later than vehicle-injected controls. **(B):** Global function of the axial muscles for trunk posture and proximal limb placement were not different between NPC and vehicle groups. **(C):** Gross sensorimotor improvement during locomotion was not observed using the BBB open field test. **(D):** Similar results were observed with the BBB subscore, a scale created to avoid the forelimb-hind limb ceiling effect (dashed line) component of the scale **(C)** but requires quadrupedal locomotion. Abbreviations: aNPC, adult neural precursor cells; BBB, Basso, Beattie and Bresnahan scale; NS, not significant.

ischemic injury and regeneration inhibition; however, unilateral contusion models do not model a clinically relevant injury [14], and unilateral or midline contusion-only models still relate poorly to injury level and severity [12, 13]. Due to these limitations to translation, the scientific community has reached consensus that translation to clinical trials for cervical SCI requires proof-of-efficacy in a cervical SCI model using a contusion-compression injury with a dose response in behavioral and nonbehavioral improvement [6, 15, 56]. The first clinical trial using cell therapy for SCI was based on preclinical data from a transection model and failed to be effective in human participants [57].

The cervical cord has unique and complex cellular circuitry in terms of pathophysiology and function, making extrapolation from results in thoracic SCI problematic. The C6 clip model exhibits a dense gliotic scar, bilateral gray matter loss, preserved rim of dysmyelinated axons, cystic cavity cordoned off by inhibitory astrogliosis, and graded deficit with level and severity of injury. However, there is greater central lesional tissue and gray matter loss than with equivalent thoracic SCI models [21, 26, 28]. Consequently, cell transplantation in a cervical injury may have distinct reparative mechanisms and thresholds. The use of a cervical-level contusion-compression injury, delayed intervention, dose response, and improvements in behavioral and nonbehavioral parameters meet a high rating for preclinical evidence [56].

Cellular Therapy for SCI

Our laboratory and others have shown consistent efficacy of NPCs for use in thoracic SCI [28, 33, 58]. These cells have been shown to be nonproliferative and do not form tumors [21, 26, 28]. More detail regarding differentiation profiles, cell survival, tissue improvement, and behavioral recovery are needed to improve the efficacy of current cell therapy. Most transplantation paradigms do not exhibit robust differentiation to mature oligodendrocytes [20, 22, 59, 60]. Within this paradigm, a greater

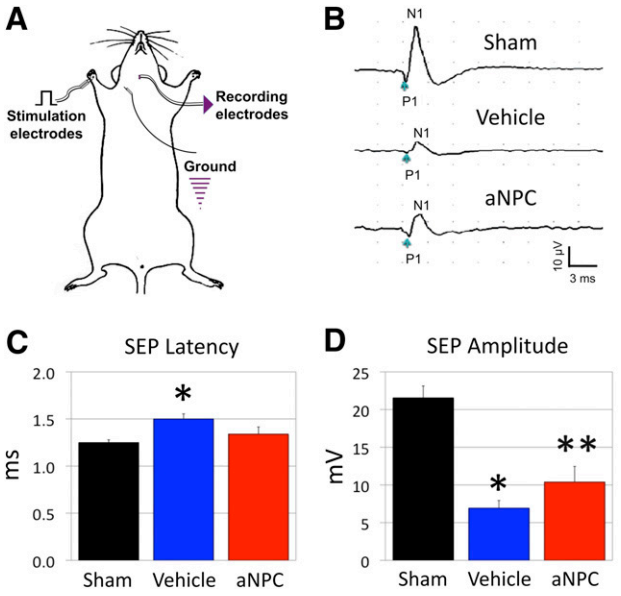

Figure 6. Forelimb neurophysiology is improved by NPC transplantation in cervical spinal cord injury. Conduction and electrophysiology of the forelimb through SEPs **(A)** was also improved following NPC transplantation (bottom) compared with vehicle injection (middle) **(B)**. The vehicle-control group exhibited prolonged latency **(C)** and decreased amplitude **(D)** compared with shams, whereas NPC-treated animals demonstrated no difference in latency and a significant improvement in amplitude of SEP nerve conduction. **(C):** *, $p < .05$ for NPC versus sham. **(D):** *, $p < .05$ vehicle versus sham; **, $p < .05$ NPC versus vehicle and sham. Abbreviations: aNPC, adult neural precursor cell; N1, negative peak inflection; P1, positive peak inflection; SEP, sensory-evoked potential.

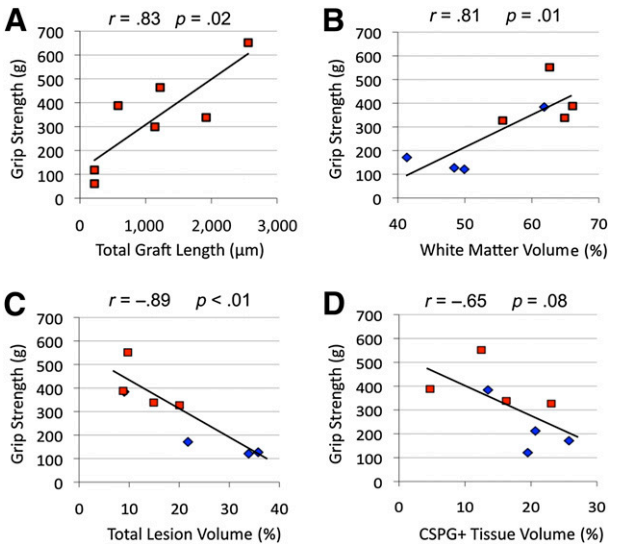

Figure 7. Correlational analysis of grip-strength recovery with respect to neural stem/precursor cell (NPC) graft, tissue sparing, and lesion formation. **(A):** Functional strength improvement following NPC engraftment was found to be strongly proportional to the length of NPC grafts. **(B):** Grip strength also exhibited a strong positive correlation to white matter present in vehicle (blue) and NPC (red) groups. **(C, D):** Forelimb strength was also found to exhibit a strong inverse relationship to total lesion volume **(C)** and a weakly negative relationship to total $CSPG^+$ extracellular matrix tissue deposition **(D)**. Additional analyses can be found in supplemental online Table 1. Abbreviation: CSPG, chondroitin sulfate proteoglycan.

proportion of neurons were observed in the cervical grafts, with the caudal grafts exhibiting a similar differentiation profile to our previous studies in thoracic SCI [21]. These increases in NPC-derived neurons and astrocytes coincided with a reduction in YFP-only cells but not mature oligodendrocytes, suggesting that the regional effects of the cervical enlargement do not inhibit oligodendrogenesis. Exactly how the microenvironment of the cervical enlargement induces this increased differentiation is not yet known, but it has been observed in similar NPC transplantation studies [59]. Clinical trials testing neural stem cell transplantation have occurred in participants with amyotrophic lateral sclerosis, and cervical injections have been well tolerated with no subsequent histological changes [61].

Immune rejection is also a considerable limiting factor in cellular transplantation [62]. Cell survival greater than 1%–5% is rarely observed in mouse-to-rat and human-to-rodent xenograft studies without the use of severely immunocompromised recipients [30, 59]; however, cell survival as low as 1% has been shown to be sufficient for white matter preservation in mice [30], whereas up to a fivefold increase in cell number was not sufficient for tissue preservation and functional recovery [59]. Given that NPC-mediated repair does not appear to be due to early trophic factor expression [26, 27], the relation between long-term graft survival and functional recovery requires more evaluation.

NPCs Confer Functional Recovery to the Forelimb

Providing evidence of improvement in forelimb function in bilateral cervical models is critical. Initial studies in cervical models failed to demonstrate tissue preservation or behavioral outcomes following NPC transplantation [18]. We report improvements in neurophysiological, behavioral, and nonbehavioral outcomes in a severe cervical contusion-compression injury following delayed NPC transplantation. The improved grip strength observed in this study suggests that NPCs may function to preserve at-level function. Interestingly, grip strength was not improved in a previous study of transplanting committed neuronal cells in bilateral cervical SCI [44], and a dose response to stem cell therapy is rarely reported. In addition, our electrophysiology data indicate that this improvement was not due to rigidity or spasticity, as has been observed previously [38]. Due to the severity of this injury model, forelimb behavioral tasks that are used routinely in hemisection studies, such as forelimb evaluation during locomotion [63], rearing in cylinder test [13], or reaching/grasping and food manipulation while standing [64], are not feasible.

Although the BBB scale is a comprehensive analysis of locomotion, it cannot evaluate forelimb deficits. The BBB subscore was used in an attempt to circumvent this; however, this scale relates to the nonlinear upper portion of the BBB scale [65] and does not appear to accommodate tetraplegic animals. The lack of sensitivity and utility of BBB scale and subscore and inclined plane in a bilateral cervical SCI model has been demonstrated elsewhere [43] and suggests that more sensitive measures of neurobehavior ought to be used in subsequent cervical studies.

Mechanism of NPC-Mediated Improvements

Endogenous progenitors have been shown to activate on central nervous system injury during the subacute phase to minimize the lesion by clearing cellular debris, sequestering the lesion by

forming a protective scar through astrogliosis, and remodeling damaged tissue [66, 67]. Cell transplantation paradigms using NPCs exploit targets of endogenous repair processes while dampening the corresponding inhibitory scarring [18].

Although it is known that glial scar disruption and remyelination contribute directly to axonal growth and neural plasticity [24, 53], these mechanisms have not been fully elucidated following cell transplantation. Axons are able to migrate through areas of reactive astrocytes, but they are halted at CSPG motifs, which are upregulated at the lesion epicenter and periphery, effectively blocking regeneration [34, 53, 68, 69]. This study demonstrates that exogenous NPCs mediate white matter preservation concurrently with reductions in the astrogliotic scar, which we have not observed following NPC transplantation in thoracic SCI [21, 26]. This suggests NPCs balance lesion containment and tissue remodeling differently and more effectively within the injured cervical cord. The distinct differentiation profiles of grafts within the cervical enlargement (rostral), along with improved neural circuit conduction, indicate that a potentially unique action is occurring within the cervical spinal cord. Although a trend toward reduced ventral horn atrophy and less total neuron loss was observed, there was no clear indication that NPCs mediated improved forelimb function through tissue preservation or indirect trophic support.

This study also delayed transplantation of NPCs until the subacute phase (2 weeks after injury), which is within a conservative therapeutic window and after the formation and maturation of gliotic scar. It has been shown by independent laboratories that cell transplantation beyond this subacute stage often is not efficacious and requires combination with other neuroprotective agents [21, 33].

Interestingly, functional recovery has been demonstrated without tissue preservation [26, 33, 38, 39], and tissue preservation has been demonstrated without functional recovery [41, 42]. Delineating underlying mechanisms of action following cell therapy may produce greater recovery following SCI.

Conclusion

The cervical enlargement offers the opportunity to analyze the forelimb and hind limb separately, permitting study of neuroplasticity at the level of injury and remyelination of coursing long tracts, respectively. More work is needed to determine the precise contribution of each potential mechanism of action that has led to the NPC-mediated repair of the injured cervical spinal cord. Interpreting efficacious recovery of the forelimb in a contusion-compression SCI model is highly translatable and should be demonstrated prior to clinical translation [6, 15, 56, 57]. This study adds to previous findings by our laboratory and others [20, 28, 33] of novel NPC-mediated effects of reduced astrogliosis, improved physiology and function in the network-rich cervical limb enlargement, and the underlying relationship between tissue modification and behavioral performance. The data presented warrant further study of cell therapy in cervical contusion-compression SCI models to determine cell-based reparative mechanisms.

Acknowledgments

We thank Jian Wang, Derrick Tam and Alyssa Lip for invaluable technical assistance, as well as Behzad Azad and Drs. Moloo, Madden, and Hanwell for expert animal care and clinical rigor. This work was supported by grants from the Canadian Institutes of Health Research (CIHR); Ontario Neurotrauma Foundation (ONF); the Krembil Family Foundation; the Halbert Chair in Neural Repair and Regeneration; and personal support from ONF (K.S.), CIHR (J.T.W.), University of Toronto master and doctoral degree programs (J.T.W.) and CREMS (J.Z., F.N.), and the McLaughlin Centre (J.T.W.).

Author Contributions

J.T.W.: conception and design, collection and/or assembly of data, data analysis and interpretation, manuscript writing, final approval of manuscript; K.S.: conception and design, collection of data, data analysis and interpretation, final approval of manuscript; J.A.Z. and F.N.: collection and/or assembly of data; M.G.F.: conception and design, financial support, final approval of manuscript.

Disclosure of Potential Conflicts of Interest

The authors indicate no potential conflicts of interest.

References

1 Cripps RA, Lee BB, Wing P et al. A global map for traumatic spinal cord injury epidemiology: Towards a living data repository for injury prevention. Spinal Cord 2011;49:493–501.

2 Wyndaele M, Wyndaele J-J. Incidence, prevalence and epidemiology of spinal cord injury: What learns a worldwide literature survey? Spinal Cord 2006;44:523–529.

3 Sekhon LH, Fehlings MG. Epidemiology, demographics, and pathophysiology of acute spinal cord injury. Spine 2001;26(suppl):S2–S12.

4 Spinal Cord Injury Facts and Statistics. Vancouver, British Columbia, Canada: Rick Hansen Spinal Cord Injury Registry, 2006.

5 Anderson KD. Targeting recovery: Priorities of the spinal cord-injured population. J Neurotrauma 2004;21:1371–1383.

6 Kwon BK, Soril LJ, Bacon M et al. Demonstrating efficacy in preclinical studies of cellular therapies for spinal cord injury - how much is enough? Exp Neurol 2013;248:30–44.

7 Kwon BK, Ghag A, Reichl L et al. Opinions on the preclinical evaluation of novel therapies for spinal cord injury: A comparison between researchers and spinal cord-injured individuals. J Neurotrauma 2012;29:2367–2374.

8 Mack GS. ReNeuron and StemCells get green light for neural stem cell trials. Nat Biotechnol 2011;29:95–97.

9 Bretzner F, Gilbert F, Baylis F et al. Target populations for first-in-human embryonic stem cell research in spinal cord injury. Cell Stem Cell 2011;8:468–475.

10 Wilcox JT, Cadotte D, Fehlings MG. Spinal cord clinical trials and the role for bioengineering. Neurosci Lett 2012;519:93–102.

11 Siegenthaler MM, Tu MK, Keirstead HS. The extent of myelin pathology differs following contusion and transection spinal cord injury. J Neurotrauma 2007;24:1631–1646.

12 Anderson KD, Sharp KG, Steward O. Bilateral cervical contusion spinal cord injury in rats. Exp Neurol 2009;220:9–22.

13 Ferguson AR, Irvine K-A, Gensel JC et al. Derivation of multivariate syndromic outcome metrics for consistent testing across multiple models of cervical spinal cord injury in rats. PLoS ONE 2013;8:e59712.

14 Tator CH. Update on the pathophysiology and pathology of acute spinal cord injury. Brain Pathol 1995;5:407–413.

15 Kwon BK, Hillyer J, Tetzlaff W. Translational research in spinal cord injury: A survey of opinion from the SCI community. J Neurotrauma 2010;27:21–33.

16 Meletis K, Barnabé-Heider F, Carlén M et al. Spinal cord injury reveals multilineage differentiation of ependymal cells. PLoS Biol 2008;6:e182.

17 Göritz C, Dias DO, Tomilin N et al. A pericyte origin of spinal cord scar tissue. Science 2011;333:238–242.

18 Tetzlaff W, Okon EB, Karimi-Abdolrezaee S et al. A systematic review of cellular transplantation therapies for spinal cord injury. J Neurotrauma 2011;28:1611–1682.

19 Ruff CA, Wilcox JT, Fehlings MG. Cell-based transplantation strategies to promote plasticity following spinal cord injury. Exp Neurol 2012;235:78–90.

20 Hofstetter CP, Holmström NAV, Lilja JA et al. Allodynia limits the usefulness of intraspinal neural stem cell grafts; directed differentiation improves outcome. Nat Neurosci 2005;8: 346–353.

21 Karimi-Abdolrezaee S, Eftekharpour E, Wang J et al. Synergistic effects of transplanted adult neural stem/progenitor cells, chondroitinase, and growth factors promote functional repair and plasticity of the chronically injured spinal cord. J Neurosci 2010;30:1657–1676.

22 Nori S, Okada Y, Yasuda A et al. Grafted human-induced pluripotent stem-cell-derived neurospheres promote motor functional recovery after spinal cord injury in mice. Proc Natl Acad Sci USA 2011;108:16825–16830.

23 Nashmi R, Jones OT, Fehlings MG. Abnormal axonal physiology is associated with altered expression and distribution of Kv1.1 and Kv1.2 K+ channels after chronic spinal cord injury. Eur J Neurosci 2000;12:491–506.

24 Bradbury EJ, McMahon SB. Spinal cord repair strategies: Why do they work? Nat Rev Neurosci 2006;7:644–653.

25 Fehlings MG, Tator CH. The relationships among the severity of spinal cord injury, residual neurological function, axon counts, and counts of retrogradely labeled neurons after experimental spinal cord injury. Exp Neurol 1995; 132:220–228.

26 Hawryluk GW, Spano S, Chew D et al. An examination of the mechanisms by which neural precursors augment recovery following spinal cord injury: A key role for remyelination. Cell Transplant 2014;23:365–380.

27 Yasuda A, Tsuji O, Shibata S et al. Significance of remyelination by neural stem/progenitor cells transplanted into the injured spinal cord. STEM CELLS 2011;29:1983–1994.

28 Karimi-Abdolrezaee S, Eftekharpour E, Wang J et al. Delayed transplantation of adult neural precursor cells promotes remyelination and functional neurological recovery after spinal cord injury. J Neurosci 2006;26:3377–3389.

29 Windrem MS, Schanz SJ, Guo M et al. Neonatal chimerization with human glial progenitor cells can both remyelinate and rescue the otherwise lethally hypomyelinated shiverer mouse. Cell Stem Cell 2008;2:553–565.

30 Bottai D, Cigognini D, Madaschi L et al. Embryonic stem cells promote motor recovery and affect inflammatory cell infiltration in spinal cord injured mice. Exp Neurol 2010;223:452–463.

31 Sharp J, Frame J, Siegenthaler M et al. Human embryonic stem cell-derived oligodendrocyte progenitor cell transplants improve recovery after cervical spinal cord injury. STEM CELLS 2010;28:152–163.

32 Cao Q, He Q, Wang Y et al. Transplantation of ciliary neurotrophic factor-expressing adult oligodendrocyte precursor cells promotes remyelination and functional recovery after spinal cord injury. J Neurosci 2010;30:2989–3001.

33 Keirstead HS, Nistor G, Bernal G et al. Human embryonic stem cell-derived oligodendrocyte progenitor cell transplants remyelinate and restore locomotion after spinal cord injury. J Neurosci 2005;25:4694–4705.

34 McKeon RJ, Schreiber RC, Rudge JS et al. Reduction of neurite outgrowth in a model of glial scarring following CNS injury is correlated with the expression of inhibitory molecules on reactive astrocytes. J Neurosci 1991;11:3398–3411.

35 Fitch MT, Doller C, Combs CK et al. Cellular and molecular mechanisms of glial scarring and progressive cavitation: In vivo and in vitro analysis of inflammation-induced secondary injury after CNS trauma. J Neurosci 1999;19: 8182–8198.

36 Bradbury EJ, Moon LD, Popat RJ et al. Chondroitinase ABC promotes functional recovery after spinal cord injury. Nature 2002;416: 636–640.

37 García-Alías G, Barkhuysen S, Buckle M et al. Chondroitinase ABC treatment opens a window of opportunity for task-specific rehabilitation. Nat Neurosci 2009;12:1145–1151.

38 Jin Y, Neuhuber B, Singh A et al. Transplantation of human glial restricted progenitors and derived astrocytes into a contusion model of spinal cord injury. J Neurotrauma 2011;28: 579–594.

39 Hooshmand MJ, Sontag CJ, Uchida N et al. Analysis of host-mediated repair mechanisms after human CNS-stem cell transplantation for spinal cord injury: Correlation of engraftment with recovery. PLoS One 2009;4: e5871.

40 Hill CE, Proschel C, Noble M et al. Acute transplantation of glial-restricted precursor cells into spinal cord contusion injuries: Survival, differentiation, and effects on lesion environment and axonal regeneration. Exp Neurol 2004;190:289–310.

41 Takami T, Oudega M, Bates ML et al. Schwann cell but not olfactory ensheathing glia transplants improve hindlimb locomotor performance in the moderately contused adult rat thoracic spinal cord. J Neurosci 2002;22: 6670–6681.

42 Pearse DD, Marcillo AE, Oudega M et al. Transplantation of Schwann cells and olfactory ensheathing glia after spinal cord injury: Does pretreatment with methylprednisolone and interleukin-10 enhance recovery? J Neurotrauma 2004;21:1223–1239.

43 Schaal SM, Kitay BM, Cho KS et al. Schwann cell transplantation improves reticulospinal axon growth and forelimb strength after severe cervical spinal cord contusion. Cell Transplant 2007;16:207–228.

44 Rossi SL, Nistor G, Wyatt T et al. Histological and functional benefit following transplantation of motor neuron progenitors to the injured rat spinal cord. PLoS One 2010;5: e11852.

45 Rivlin AS, Tator CH. Objective clinical assessment of motor function after experimental spinal cord injury in the rat. J Neurosurg 1977; 47:577–581.

46 Dolan EJ, Tator CH. A new method for testing the force of clips for aneurysms or experimental spinal cord compression. J Neurosurg 1979;51:229–233.

47 Joshi M, Fehlings MG. Development and characterization of a novel, graded model of clip compressive spinal cord injury in the mouse: Part 1. Clip design, behavioral outcomes, and histopathology. J Neurotrauma 2002;19:175–190.

48 Wilcox JT, Fehlings MG. The acute clip contusion-compression model of cervial spinal cord injury in the ratExperimental Neurology in Animals Models. In: Janowski M, edSecaucus, NJ: Springer, Humana Press, 2013.

49 Nguyen DH, Cho N, Satkunendrarajah K et al. Immunoglobulin G (IgG) attenuates neuroinflammation and improves neurobehavioral recovery after cervical spinal cord injury. J Neuroinflammation 2012;9:224.

50 Eftekharpour E, Karimi-Abdolrezaee S, Wang J et al. Myelination of congenitally dysmyelinated spinal cord axons by adult neural precursor cells results in formation of nodes of Ranvier and improved axonal conduction. J Neurosci 2007;27:3416–3428.

51 Lankhorst AJ, ter Laak MP, van Laar TJ et al. Effects of enriched housing on functional recovery after spinal cord contusive injury in the adult rat. J Neurotrauma 2001;18:203–215.

52 Bradbury EJ, Carter LM. Manipulating the glial scar: Chondroitinase ABC as a therapy for spinal cord injury. Brain Res Bull 2011;84: 306–316.

53 Silver J, Miller JH. Regeneration beyond the glial scar. Nat Rev Neurosci 2004;5:146–156.

54 Anderson KD, Abdul M, Steward O. Quantitative assessment of deficits and recovery of forelimb motor function after cervical spinal cord injury in mice. Exp Neurol 2004;190: 184–191.

55 Anderson KD, Gunawan A, Steward O. Quantitative assessment of forelimb motor function after cervical spinal cord injury in rats: Relationship to the corticospinal tract. Exp Neurol 2005;194:161–174.

56 Kwon BK, Okon EB, Tsai E et al. A grading system to evaluate objectively the strength of pre-clinical data of acute neuroprotective therapies for clinical translation in spinal cord injury. J Neurotrauma 2011;28:1525–1543.

57 Lammertse DP, Jones LA, Charlifue SB et al. Autologous incubated macrophage therapy in acute, complete spinal cord injury: Results of the phase 2 randomized controlled multicenter trial. Spinal Cord 2012;50:661–671.

58 Cummings BJ, Uchida N, Tamaki SJ et al. Human neural stem cells differentiate and promote locomotor recovery in spinal cord-injured mice. Proc Natl Acad Sci USA 2005;102: 14069–14074.

59 Piltti KM, Salazar DL, Uchida N et al. Safety of epicenter versus intact parenchyma as a transplantation site for human neural stem cells for spinal cord injury therapy. STEM CELLS TRANSLATIONAL MEDICINE 2013;2:204–216.

60 Abematsu M, Tsujimura K, Yamano M et al. Neurons derived from transplanted neural stem cells restore disrupted neuronal circuitry in a mouse model of spinal cord injury. J Clin Invest 2010;120:3255–3266.

61 Feldman EL, Boulis NM, Hur J et al. Intraspinal neural stem cell injections in ALS subjects: Phase I trial outcomes. Ann Neurol 2014; 75:363–373.

62 Anderson AJ, Haus DL, Hooshmand MJ et al. Achieving stable human stem cell engraftment and survival in the CNS: Is the future of

regenerative medicine immunodeficient? Regen Med 2011;6:367–406.

63 Singh A, Krisa L, Frederick KL et al. Forelimb locomotor rating scale for behavioral assessment of recovery after unilateral cervical spinal cord injury in rats. J Neurosci Methods 2014;226:124–131.

64 Whishaw IQ, Pellis SM, Gorny B et al. Proximal and distal impairments in rat forelimb use in reaching follow unilateral pyramidal tract lesions. Behav Brain Res 1993;56:59–76.

65 Ferguson AR, Hook MA, Garcia G et al. A simple post hoc transformation that improves the metric properties of the BBB scale for rats with moderate to severe spinal cord injury. J Neurotrauma 2004;21:1601–1613.

66 Rowland JW, Hawryluk GWJ, Kwon B et al. Current status of acute spinal cord injury pathophysiology and emerging therapies: Promise on the horizon. Neurosurg Focus 2008;25:E2.

67 Hughes EG, Kang SH, Fukaya M et al. Oligodendrocyte progenitors balance growth with self-repulsion to achieve homeostasis in the adult brain. Nat Neurosci 2013;16:668–676.

68 Hunanyan AS, García-Alías G, Alessi V et al. Role of chondroitin sulfate proteoglycans in axonal conduction in mammalian spinal cord. J Neurosci 2010;30:7761–7769.

69 Davies SJ, Goucher DR, Doller C et al. Robust regeneration of adult sensory axons in degenerating white matter of the adult rat spinal cord. J Neurosci 1999;19:5810–5822.

See www.StemCellsTM.com for supporting information available online.

